ROYAL SOCIETY
OF CHEMISTRY

PAPER

Check for updates

TOF-SIMS analysis of curcuminoids and curcumin crystals crystallized from their pure and impure solutions†

K. Vasanth Kumar, [iD] ‡*[ab] Claire Heffernan,§[a] Kiran A. Ramisetty, [iD] ¶[a]
Christopher A. Howard [iD] [c] and Sergey Beloshapkin‡[a]

Impurities are frequently encountered during the crystallisation of active pharmaceutical compounds. Impurities can either adsorb onto active sites or replace atoms of the crystal lattice. Locating the impurities, especially structurally-similar impurities, on the crystal surface is challenging. In this work, we showed that time-of-flight secondary ion mass spectrometry (TOF-SIMS) can be successfully used to simultaneously quantify the composition of the two structurally-similar impurities, demethoxycurcumin (DMC) and bisdemethoxycurcumin (BDMC), on the surface of the curcumin (CUR) crystals obtained from crystal growth and cooling crystallisation experiments. The distribution of the three curcuminoids on the crystal surface was evaluated through imaging of the specific ions that correspond to intact molecules of the curcuminoids. In terms of location, both BDMC and DMC were evenly distributed on the surfaces of the facets of the curcumin crystals. Additionally, we found that BDMC and DMC occupy their own sites or they are located on the same site on the crystal surface providing evidence for lattice replacement of these molecules. Thus our results demonstrate the potential of TOF-SIMS to provide new information that can help to understand crystallisation.

1. Introduction

Structurally-similar impurities frequently appear during the crystallization of a number of important industrial compounds. Such impurities often introduce undesirable effects that includes the modification of the crystal habit, increased mosaicity, altered crystal growth rate, and can ultimately decrease the purity of the final crystals.[1–5] Additionally, structurally similar impurities can also replace atoms on the crystal lattice, modifying its intrinsic properties.[6,7] Depending on the type and nature of the impurities, as well as experimental conditions, impurities can alter the properties of the final crystals in terms of the crystal structure, and even other commonly encountered factors such as

crystal agglomeration, attrition, overall crystal morphology, and yield.[2,8,9] An understanding of the impurity inclusion process is essential for optimising process design, improving the product yield, upscaling the growth process or predicting the growth properties of other related crystals. Understandings on the impurity inclusion mechanism is absolutely essential to understand the fundamentals of crystallisation that includes nucleation and crystal growth. During the nucleation process, impurities can alter the surface energy and the pre-exponential factors and consequently the nucleation rate.[19] Impurity inclusion or adsorption on the crystal surface can alter the surface energy and thus can either increase or decrease the crystal growth rate.[10] Identifying the location of impurities on the bulk crystal can shed new light on the impurity inclusion mechanism and its effect on the crystallisation kinetics and thermodynamics. The effect of impurities on the crystallisation process have been discussed in detail in several literature reviews.[8,11,12]

Typically, chromatographic techniques are employed to quantify the amount of impurities being incorporated into the crystals. Bulk changes induced by impurities can be determined using X-ray diffraction and using a range of spectroscopic techniques. To fully elucidate the effects of impurities during crystal growth, information about the location of impurities is necessary. Impurities can be surface selective and can preferentially adsorb onto a specific crystal face or replace a specific crystallographic plane.[12] It is

[a] *Synthesis and Solid State Pharmaceutical Centre and Bernal Institute, University of Limerick, Ireland. E-mail: vasanth.kannuchamy@ul.ie*
[b] *Pharmaceutical Manufacturing Technology Centre (PMTC), University of Limerick, Ireland*
[c] *Department of Physics & Astronomy, University College London, London, WC1E 6BT, UK*

‡ Equal contribution.
§ Present address: AstraZeneca, Charter Way, Macclesfield SK10 2NA, United Kingdom.
¶ Present address: MSD Ballydine, Kilsheelan, Clonmel, Co Tipperary, Ireland.

experimentally challenging to map the location of impurities on the crystal surface when dealing with structurally-similar impurities. For instance, widely-used techniques such as X-ray photoelectron spectroscopy (XPS) and energy-dispersive X-ray spectroscopy (EDX) cannot provide direct information about the surface distribution of structurally-similar impurities at the molecular level. Likewise, spectroscopic techniques such as Raman spectroscopy also suffer from similar limitations, unless the impurities directly affect the vibrational modes of the bulk crystal. The use of these techniques becomes ambiguous, especially if we have deal with the presence of more than one impurity which may be structurally similar to the crystallizing compound.[13]

In this context, TOF-SIMS can be a potentially useful technique and can provide high-quality information about the impurity locations on the surface of a bulk crystal, especially while dealing with structurally-similar impurities. More importantly, TOF-SIMS can also provide a chemical map with specificity, detection limit and resolution that matches the resolving power of mass spectrometry.[14] The imaging can be performed at a spatial resolution that can expose the location of the adsorbed impurities on the crystal surface or even in the bulk of the crystal. TOF-SIMS has already been used to characterize polymeric and biological samples.[15–19] The detailed working principles and the advantages of SIMS can be found in the work of Liebl.[20] TOF-SIMS is a retrospective technique and enables detailed post-acquisition analysis to get in-depth molecular information.[21,22] TOF-SIMS is considered as a process analytical technique during manufacturing of pharmaceutical products for root cause investigations. The application of TOF-SIMS in the pharmaceutical sector is reviewed by Barnes *et al.*[23] TOF-SIMS remains a state-of-the-art technique and one of the few that can spatially resolve chemical data of organic compounds and can connect with the morphological aspects of the materials of interest.

In this work, we exploit the ability of TOF-SIMS to connect chemical data to sample morphology and map the distribution of two structurally-similar impurities, bisdemethoxycurcumin (BDMC) and desmethoxycurcumin (DMC), in the final product of curcumin (CUR) crystals crystallized from their impure solutions. This system is purposely chosen as the molecular structure of the impurities is similar to that of the crystallizing compound (see Fig. 1) and their molecular weight differs from each other only by a few grams per mole (molecular weight of CUR: 369 g mol⁻¹, DMC: 339 g mol⁻¹, BDMC: 309 g mol⁻¹), containing the same types of atoms, functional groups and chemical coordination. This means that commonly-used techniques like XPS and EDX cannot be implemented to probe the material for the impurities. Also, this system is particularly difficult to probe with spectroscopic techniques like Raman spectroscopy as here all the structurally-similar molecules add-up to the intensity of scattered light and there is no straightforward technique to deconvolute the spectra in order to obtain quantitative information about the percentage of the
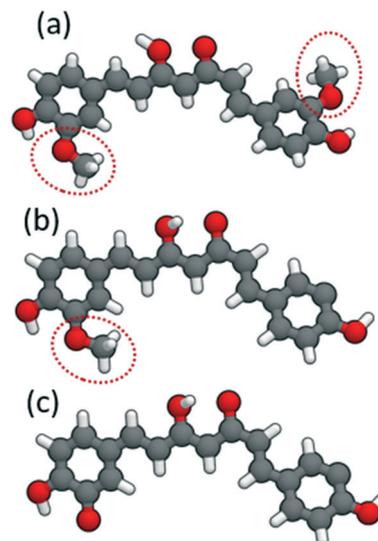

Fig. 1 Structures of the structurally-similar curcuminoids, (a) CUR, (b) DMC, and (c) BDMC (the methyl groups shown within the dotted circles show the structural difference between the three curcuminoids).

impurities, especially their location in the sample. Furthermore, Raman spectroscopy requires stable instrument conditions, homogeneous solid properties of the different samples, and similar measurement conditions that include laser power, irradiation time, spectral resolution, number of acquisitions, and even sample orientation. Additionally, the present system CUR grows as needles or as spherulites composed of near micron sized filaments. A frequently encountered problem during the growth of curcumin is the outgrowth of new crystals on the surface of the growing single crystal. This makes it even more difficult to chemically map the surface of the growing face using spectroscopic techniques. TOF-SIMS will be a complementary and ideal technique to deal with this type of system as it can chemically map the crystal surface at the micron scale and at the molecular level; it can expose the atomic/molecular components in the system and thus does not require any supervised learning or chemometrics.[20] More importantly, it can provide a discrete, high-resolution chemical map of the target compound curcumin and the two other impurities on the surfaces of the crystals. Additionally, a high-resolution chemical map of the molecules of interest can be obtained for several crystals to few crystals or even a specific facet (if required) of a particular crystal by operating TOF-SIMS in spectroscopy mode or in imaging mode. Spectroscopy mode gains information about the bulk product as a large area can be mapped for its chemical composition, whereas in imaging mode the quality of up to a single crystal can be exclusively probed and the locations of the impurities can be identified. In this work, we operated TOF-SIMS in both spectroscopy and image modes, to quantify the concentration of the two structurally similar compounds, BDMC and DMC, on the surface of the form I (FI) curcumin crystals and a new form of curcumin spherulite. We also provided the TOF-SIMS

reference spectra for the pure CUR and the two other impurities DMC and BDMC, which can be added to chemical libraries. The purpose of this work is to show how TOF-SIMS can be used to map the spatial distribution of the two structurally similar impurities on the surface of the bulk crystals obtained from cooling crystallisation and crystal growth experiments. We compare the results obtained from HPLC and discuss how these techniques will complement each other and provide useful information to crystallisation scientists. Additionally, we discuss the advantages, limitations and practical difficulties that we encountered while using this technique to characterise the surface concentration of impurities. Finally, based on the TOF-SIMS results, we made key theoretical arguments to explain the influence of structurally-impurities on the nucleation and crystal growth kinetics of the studied model compound curcumin in the presence of structurally-similar impurities.

2. Experimental section

2.1. Materials

Commercial grade crude curcumin (Crude_CUR) was purchased from Merck (as specified by the manufacturer: CUR > 75% nominal purity; HPLC, area %; containing <20% demethoxycurcumin and <5% bisdemethoxycurcumin). Isopropanol (99.9% purity) was purchased from Acros Organics.

2.2. Sample preparation

To demonstrate the potential and sensitivity of TOF-SIMS and for reliable data interpretation, we carefully prepared the solid samples using different methods and the experimental protocols described below:

2.2.1. Preparation of standard pure components of curcuminoids. The pure components of the three curcuminoids, CUR, DMC and BDMC, in their amorphous forms were obtained with gravity column chromatography using an earlier developed method.[24] These samples are labelled as CUR_s, DMC_s and BDMC_s, respectively, where 's' refers to 'standard' samples. These samples are used as standards to record the TOF-SIMS spectra of the curcuminoids.

2.2.2. Single crystals of pure curcumin. Pure curcumin was obtained *via* five successive cooling crystallization experiments. All the recrystallization experiments were performed by dissolving a known mass of the as-received crude curcumin in 1 litre of isopropanol solvent. During each stage of the recrystallization experiments, the initial concentration of curcumin was set to 4.72 g L^{-1} which is equivalent to the solubility of curcumin in IPA at ~60 °C. The solids were dissolved at 70 °C (10 °C above the solubility temperature) for 45 minutes, after which the solution was cooled to the working temperature of 10 °C at a rapid cooling rate of 8 °C min^{-1}. Unless specified, all the re-crystallization experiments were performed in a 100 mL reactor using an EasyMax Mettler Toledo Workstation and at a constant

agitation speed (using an over-head stirrer) of 250 RPM. The solvent volume was adjusted according to the purity of the final product obtained after each recrystallization batch. The crystal collected from the final recrystallization batch was labelled as CUR_n, where 'n' refers to the needle shaped habit of the final crystallized product.

2.2.3. Single crystals of curcumin needles of nominal purity from impure solution. 0.6 g of the as-received commercial grade crude curcumin was dissolved in 100 mL of isopropanol solvent at 70 °C for 45 minutes. Based on the purity, this should give a curcumin solution of concentration 4.72 g L^{-1} plus a DMC concentration of 1.07 g L^{-1} and BDMC concentration of 0.22 g L^{-1}. This solution was rapidly cooled to a working temperature of 20 °C at a cooling ate of 8 °C min^{-1}. This should produce a supercooled solution ($\Delta T = T - T^* = 60 - 20 = 40$ °C) with an initial supersaturation of $S = 5.614$ at 20 °C. Then the solution was maintained at this temperature for 48 hours to ensure complete consumption of supersaturation. Nucleation is observed roughly after six hours, and this batch produces needle shaped crystals. The samples were collected after 48 hours and filtered using a vacuum filter. The filtrate was then washed with an isopropanol/water (70/30 v/v) solvent mixture eight to ten times, after which the wash liquids were almost colourless. The washed samples were then dried at 60 °C for 48 hours and then stored in glass vials wrapped with aluminium foil. The sample was labelled as CUR_n_impure.

2.2.4. Curcumin spherulites of high purity from impure solution. 0.6 g of the as-received commercial grade crude curcumin was dissolved in 100 mL of isopropanol solvent at 70 °C for 45 minutes. As mentioned above, this solution should contain CUR, DMC and BDMC of concentration 4.8 g L^{-1}, 1.07 g L^{-1} and 0.22 g L^{-1}, respectively. We rapidly cooled this solution to a working temperature of 5 °C at a cooling rate of 8 °C min^{-1}. This should produce a supercooled solution ($\Delta T = T - T^* = 60 - 5 = 55$ °C) with an initial supersaturation of $S > 6$. Then the solution was maintained at this temperature for 48 hours to ensure complete consumption of supersaturation. Nucleation was observed roughly after eight hours, and this batch produced spherulites. The samples were collected after 72 hours and filtered using a vacuum filter. The filtrate was then washed with an isopropanol/water (70/30 v/v) solvent mixture eight to ten times, after which the wash liquids were almost colourless. The washed samples were then dried at 60 °C for 48 hours and then stored in glass vials wrapped with aluminium foil. This sample was labelled as CUR_sph.

2.2.5. Crystal growth of pure curcumin crystals in impure solution. 0.18 of crude curcumin was dissolved in 20 mL of IPA at 70 °C in 30 mL glass vials for 45 minutes in a water bath. Agitation was provided using a magnetic pellet. Then the vial was transferred to another bath maintained at 25 °C. This should give a supersaturation ratio, $S = c/c^* = 4.8$. Once the solution reached 25 °C, the magnetic pellet was removed from the vial and the solution was seeded with the pure curcumin crystals (CUR_n) obtained from the above batch.

The uncapped vials were then kept at 25 °C for 24 hours leaving the solution undisturbed. After 24 hours, the crystals were collected from the vials and washed with an isopropanol/water (30/70 v/v) solvent mixture eight to ten times, after which the wash liquids were almost colourless. The crystals were then dried at 60 °C for 48 hours. This experimental design excludes agitation of the solution and is purposely chosen to mimic the crystal growth of a pure crystal in impure solutions, to retrieve the seeded crystals without any breakage and to obtain good quality needle shaped crystals. The final crystalline sample was labelled as CUR_cg, where, 'cg' refers to the samples obtained from the crystal growth experiment.

2.3. TOF-SIMS measurements and data acquisition

The TOF-SIMS measurements were performed using a TOF-SIMS 5 instrument (ION-TOF GmbH, Muenster, Germany). For high lateral resolution and imaging as well as high mass resolution surface spectroscopy, this instrument is equipped with a 30 keV, three-lens BiMN cluster liquid metal ion gun. All the analysis was performed with Bi_3^+ primary ions in the positive mode and with a cycle time of 5 μs. The field of view of analysis was either 300 × 300 μm^2 or 130 × 130 μm^2 with each image containing 128 × 128 pixels; each of these pixels contains the entire mass spectrum. The analysis time was approximately 250 seconds or set to 5012 primary ions per cm^2. This specific set-up allows acquisition of images with an expected lateral resolution of 3–5 μm.

To generate the reference spectra of the curcuminoids, a small quantity of the pure components of the curcuminoids (CUR_s, DMC_s and BDMC_s) was dissolved in excess of isopropanol in order to obtain a dilute solution of the pure compounds. The diluted solution was then immediately drop-cast onto a clean aluminium foil using a plastic dropper. The solution was then allowed to dry completely on the aluminium foil before TOF-SIMS analysis. The TOF-SIMS spectra of all the other samples were obtained by depositing the solids directly on sticky tape mounted on a carbon substrate.

TOF-SIMS data analysis was performed both during acquisition and post-acquisition using the collected raw data. Data analysis was performed with the SURFACELAB 6.7 software (ION-TOF Gmbh) using the signals of CH_3^+ (m/z 15.022927), $C_2H_3^+$ (m/z 27.022927), and $C_4H_7^+$ (m/z 55.04227) for internal mass calibration. During real-time, the concentration of the three curcuminoids was recorded based on the known priori, intense molecular ion peak that represents the intact molecules of CUR, DMC and BDMC. Further interpretation of the collected spectra and the peak assignments of the molecular fragments to test the presence of any impurities (like silica in the samples) were performed during the post-acquisition stage. The total ion yield was significantly low in the imaging mode and thus the TOF-SIMS spectra of the crystalline materials were mostly obtained in spectroscopic mode. The imaging mode was chosen only on few occasions in order to expose the chemical features and how they are distributed on the crystal surface at the near micron level.

2.4. Characterization of the solid samples

The morphological features of the curcumin particles were analysed using SEM. The solid samples were transferred onto the carbon tape mounted on an SEM stage. Samples were coated with gold for 1 minute and the images were obtained using an SU70 Hitachi FEG-SEM. The concentration of the curcumin and curcuminoids in the samples was analysed using HPLC (HPLC Agilent Technologies 1260 Infinity Series) based on the procedure reported elsewhere.[16]

3. Results and discussion

3.1. Morphological analysis of the solid materials

Before probing the solid surfaces for their impurity concentration using TOF-SIMS, the crystals obtained from the recrystallization experiments and the crystals obtained from the crystal growth experiment were characterized using SEM techniques. Fig. 2 shows that the one-time recrystallized CUR (CUR_n_impure) and the five time recrystallized CUR (CUR_n) crystals from their lower grades seem to possess the expected needle shaped crystal habit. Likewise, the pure needle shaped crystals grown in impure solution (CUR_cg) retains the needle shaped crystal habit. For the case of spherulites (CUR_sph), they are composed of several nanometre to near micron thick filaments. This type of structure appears from time to time in the crystallization literature mostly in the products crystallized in the presence of stabilizing agents, mineralisation from viscous magmas, inorganic compounds from melts, inorganic crystals crystallising from impure solution and more frequently during the crystallisation of polymeric compounds.[25–32] Briefly, microscopy images confirmed the presence of two different types of spherulites, which are commonly referred to as type 1 (fully developed spherulites) and type 2 (bow-tie shaped) spherulites.[25,30,33,34] These structures exhibit a crystallographic hierarchy as they are composed of a few nanometer thick crystallites with a filament-like structure of roughly 20–30 microns and the overall size of the spherulite particles is roughly around 80–100 microns. The formation mechanism of spherulites, their structural details or the effect of process conditions on the final morphology of the crystals can be found elsewhere.[33] However, as discussed in the following sections, in this work we show that TOF-SIMS can bring quantitative information about the impurity distribution on a perfect single crystal surface and in a highly complex structure like the ones observed in spherulites. For the case of crude CUR (not shown), there is no morphological feature that can be noticed at the micron scale. This can be expected as the as-received material from the manufacturer is completely pulverized. For the convenience of the readers, in Table 1, we show the experimental conditions, crystal
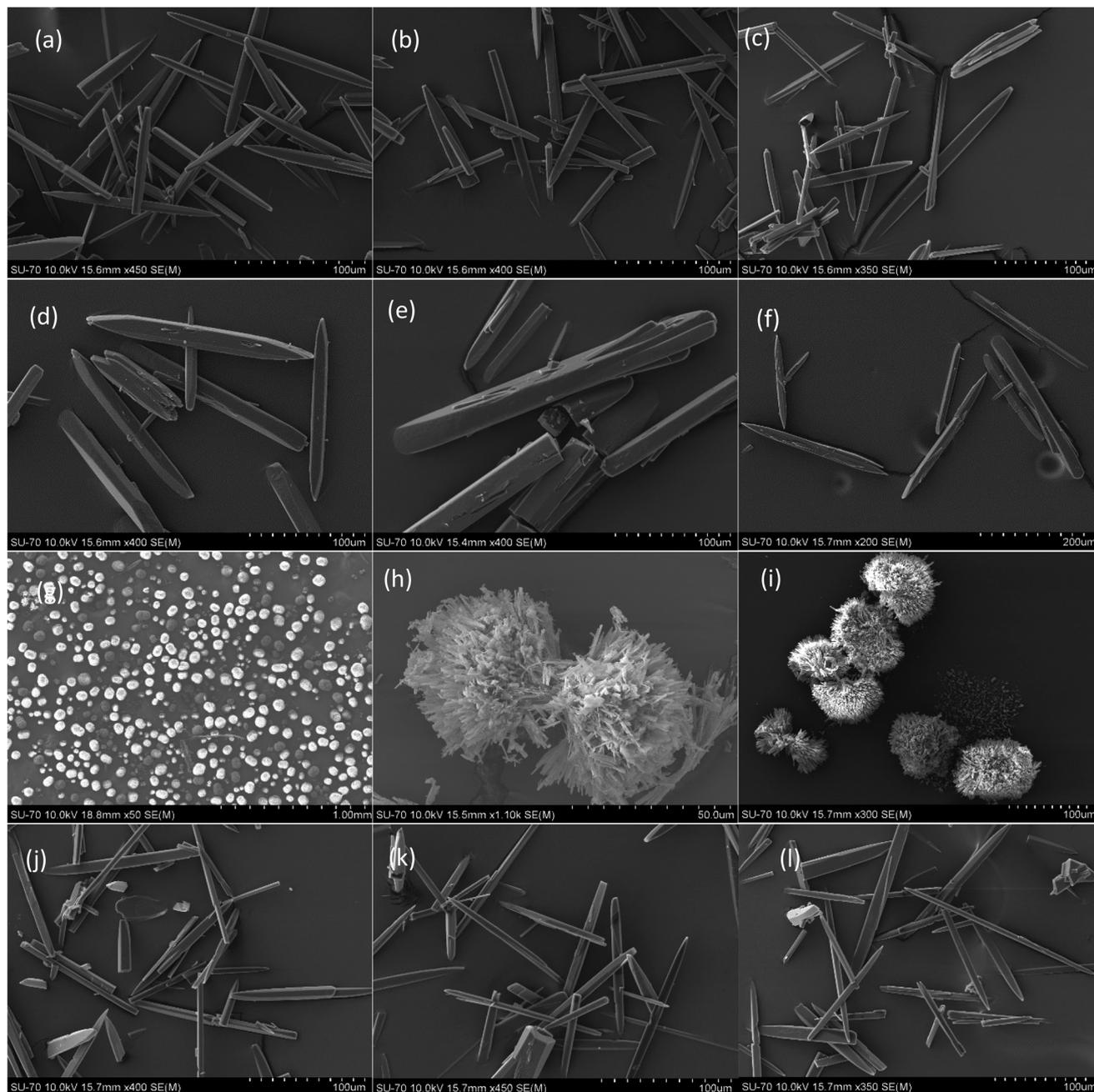
Fig. 2 SEM images of the (a–c) pure crystals of curcumin obtained from a crude curcumin solution *via* five successive recrystallisation (cooling crystallisation) experiments (CUR_n), (d–f) curcumin crystals of nominal purity obtained from a crude solution *via* cooling crystallization (CUR_n_impure), (g–i) curcumin spherulis of high purity obtained from the crude product *via* recrystallisation from a highly supercooled solution (CUR_sph), and (j–l) final crystals of curcumin grown (CUR_cg) in an impure solution (crystals were grown using a slow evaporation technique). Note: the purity level of the all crystals was determined using HPLC, and is discussed in section 3.2.

structure and morphology of the final solid materials obtained *via* crystallisation.

3.2. HPLC analysis of the solids obtained *via* nucleation

In Table 2, we show the percentage composition (by weight) of the three curcuminoids present in all the solid samples determined using the HPLC technique. The as-received crude

CUR contains up to 78.6 wt% of CUR, 17.7 wt% of DMC and 3.6 wt% of BDMC. These values slightly differ from the supplier specifications (see section 2.1.). Both the spherulites and the five-time recrystallized needle shaped curcumin crystals contain trace quantities of DMC and practically no BDMC is detected. The HPLC analysis of DMC and BDMC solids obtained *via* preparative column chromatography confirmed that they are pristine and do not contain any other

Table 1 Experimental details, crystalline structure and morphology of the final solid products

Experimental detail	Final morphology	Crystal structure[a]
Three curcuminoids, CUR, DMC and BDMC (see section 2.2.1.)	Featureless structures (not shown or discussed in this work)	—
Single crystals of pure curcumin (see section 2.2.2.)	Needles (Fig. 2a–c)	FI
Single crystals of nominal purity (see section 2.2.3.)	Needles (Fig. 2d–f)	FI
Spherulites of high purity (see section 2.2.4.)	Spherulites (Fig. 2g–i)	New form of curcumin
Crystals obtained from crystal growth experiments (see section 2.2.5.)	Needles (Fig. 2j–l)	FI

[a] Crystalline structure was determined using PXRD. The PXRD analysis of the needle shaped and the curcumin spherulites is described in detail in our recent work.[33]

curcuminoids. In this work, the HPLC chromatogram of CUR_cg was not purposely shown in Table 2 as the results obtained from TOF-SIMS. The main purpose of performing the HPLC analysis is to compare the results obtained from TOF-SIMS with the HPLC obtained values. Another objective is to show the complementarity of these techniques. It should be remembered that TOF-SIMS is a surface sensitive technique, typically characterises only the very first few atomic layers and can probe a depth of few nanometres, typically in the range of 2 to 5 nm. As we will show later, TOF-SIMS can provide information about the location of the impurity at atomic resolution on the crystal surface. On the other hand, HPLC is typically used to characterise the bulk of the crystal. Thus, care must be taken when comparing the results obtained from TOF-SIMS with HPLC. For instance, the crystals grown in an impure solution can be characterised using the TOF-SIMS technique; however, the results cannot be compared with the results obtained from the HPLC technique. The crystal growth experiments were performed with pure curcumin crystals as seeds. During the slow evaporation, it is more likely that the structurally similar impurities are adsorbed on the surface of the crystals or even incorporated into the crystal lattice. Thus, at the end of the crystal growth experiments, a typical analysis of the final crystals with HPLC should give information about the concentration of curcumin in the bulk of the crystals. On the other hand, TOF-SIMS can only provide information about the concentration of CUR, DMC and BDMC on the topmost surface (typically, few monolayers) of the crystals (CUR_cg)

grown in the impure solutions. Clearly, the pure crystals grown in impure solution should contain significant amounts of DMC and BDMC that should differ from the bulk of the sample and thus cannot be compared with the results obtained from TOF-SIMS.

3.3. Reference TOF-SIMS spectra and TOF-SIMS ion images of CUR, DMC and BDMC

In order to perform a quantitative interpretation of the TOF-SIMS data of the crystals that contain structurally similar impurities, reference spectra were obtained for the three pure components, CUR, DMC and BDMC. To collect the reference spectra, we recorded the positive TOF-SIMS spectra of the pure compounds obtained *via* preparative column chromatography. Earlier we showed that, according to the HPLC results, these samples contain only pure components and are free of other impurities. Additionally, for the case of CUR, a reference TOF-SIMS spectrum of pure CUR obtained from the five time recrystallized curcumin was collected and compared with that of the pure curcumin obtained *via* the preparative column chromatographic technique. Despite the chemical libraries provided by the instrument manufacturers and standard reference books with the reference spectra for numerous chemicals, little is known about the three curcuminoids studied in this work. The positive ion TOF-SIMS spectrum of each of the pure components (curcuminoids standards) of CUR, DMC and BDMC is shown in Fig. S1 of the ESI.† In the ESI,† we also provide the original

Table 2 HPLC determined percentage composition of CUR, DMC and BDMC in the solid samples obtained from crystallisation and column chromatography experiments (na: not analysed, nd: not detected)

Sample	HPLC obtained values			TOF-SIMS obtained values		
	CUR (wt%)	DMC (wt%)	BDMC (wt%)	CUR (wt%)	DMC (wt%)	BDMC (wt%)
Crude CUR	78.6	17.8	3.6	9.56 ± 1.07	24.06 ± 1.01	66.38 ± 2.08
CUR_s	100	nd	nd	97.9 ± 1.95	1.74 ± 0.05	0.36 ± 0.01
DMC_s (dmc1)	nd	100	Trace	23.7 ± 0.33	75.1 ± 1.43	1.1 ± 0.02
BDMC_s (bdmc1)	100	Trace	nd	1.27 ± 1.4	7.81 ± 0.09	90.92 ± 1.64
CUR_n	100	nd	nd	6.1 ± 0.58	5.26 ± 0.45	86.64 ± 1.02
CUR_n_impure	92.28	7.72	nd	3.74 ± 1.04	21.41 ± 0.39	74.86 ± 0.73
CUR_sph	100	nd	nd	4.5 ± 0.2	11.4 ± 0.29	84.1 ± 0.33
CUR_cg	na	na	na	9.56 ± 1.07	24.06 ± 1.01	66.38 ± 2.08

data of the TOF-SIMS spectra of these standard samples. All the three curcuminoids show an intense molecular ion peak that represents the intact molecule and several (less intense) signals at lower mass values that correspond to fragment ions. The molecular ion peak $[M + H]^+$ of CUR, BDMC, DMC was detected at 309 amu, 339 amu and 369 amu, respectively. For the convenience of the readers, in Fig. 3a, we separately show the major TOF-SIMS signals that should correspond to the mass (m/z) of the intact molecules and the fragment ions. The unique peak $[M + H]^+$ at 327 amu is observed only in the pure CUR sample; this can be assigned to the fragment ion of the curcumin molecule. Based on the peak area, the fragment ion peaks can be assigned to the studied compounds. Based on the peak area, the peaks $[M + H]^+$ at 189 and 107 amu can be assigned to the fragment ions of BDMC and DMC and thus can be used to get the chemical map of the impurities alone. Likewise, merely based on the peak area, the peaks $[M + H]^+$ at 73, 137 and 177 can be assigned to the fragment ions of DMC and CUR; these peaks can be used to probe the distribution of these two compounds as a whole on the crystal surface. The peak $[M +$

$H]^+$ at 147 amu is sensitive to the primary ions and the peak area is notably high in all the three curcuminoids. These peak values are assigned only based on the magnitude of the calculated peak area without performing any secondary manipulations like normalization with respect to the area under a specific molecular ion peak or under a molecular fragment ion peak. The area under the peak $[M + H]^+$ at 107 amu is relatively lower for CUR_s when compared to the calculated peak areas of $[M + H]^+$ at 147, 177 and 369 amu. Meanwhile the calculated peak area of $[M + H]^+$ at 107 amu for DMC_s and BDMC_s is significantly higher. Based on this observation, we presume that this peak can characterize the presence of the impurities DMC and BDMC on a crystal surface. The different peaks corresponding to the fragment ions assigned to the curcuminoids based on this simplistic assumption agree with the studies of Berzin et al.[35] and Coorey and Håkansson.[36] Berzin et al.'s work was based on the electron impact ionization mass spectrum of curcumin and the two other curcuminoids DMC and BDMC. Based on the assigned peak values of the fragment ions, a chemical map specific to impurities alone can be obtained. In fact, the
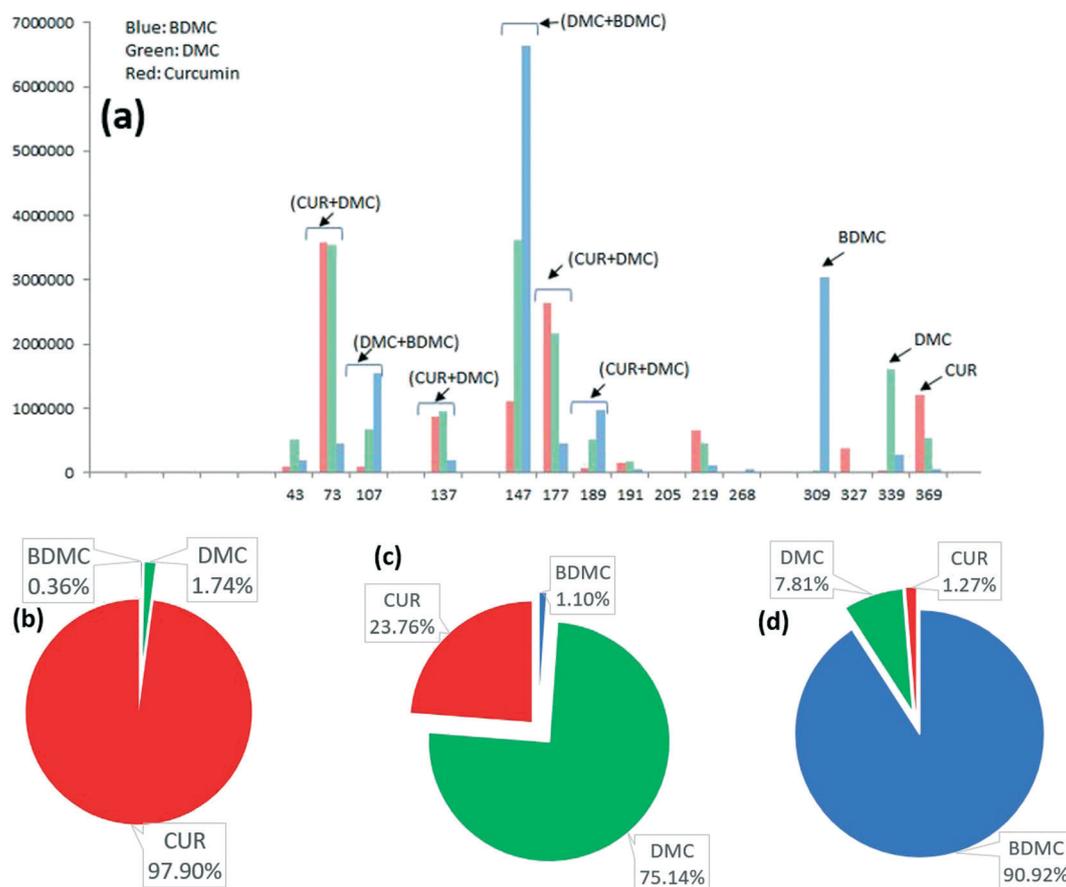

Fig. 3 (a) Peak area (shown on the x-axis) of the major TOF-SIMS signals (m/z, shown on the y-axis) of the standards, pure CUR (CUR_s), pure DMC (DMC_s) and pure BDMC (BDMC_s). For the convenience of the reader, we only show the major signals of the standard curcuminoids on the x-axis. Pie chart showing the peak area percentage of the molecular ion peak in the reference samples (red: CUR, blue: BDMC and green: DMC): (b) CUR_s (c) DMC_s, and (d) BDMC_s. Note: the percentage weight of the curcuminoids was obtained by taking an average of the areas of the molecular ion peaks obtained at five spots per sample across three samples (the standard deviation for all the three curcuminoids was always less than 2 wt% when compared to that of the average wt% of each curcuminoid in each sample).

fragment ion peak $[M + H]^+$ at 107 amu can be used to represent two of the structurally similar impurities as its contribution in pure CUR is only in trace quantities.

Despite the fact that the samples were prepared with extra care, the molecular ion peak $[M + H]^+$ of CUR was detected in the two other curcuminoid samples, DMC_s and BDMC_s. Likewise, the molecular ion peak $[M + H]^+$ of the curcuminoids can be detected but in a negligible amount in CUR_s. Based on the ratio of the peak area that corresponds to intact molecules of the three studied compounds, we found that CUR (m/z = 369) is present only in trace amounts in the reference curcuminoid sample, BDMC_s, and >20% in DMC_s (shown as a pie-chart in Fig. 3b–d; see also Table 2 where we showed the TOF-SIMS obtained weight percentage of the curcuminoids in CUR_s, DMC_s and BDMC_s). The pure CUR carefully obtained *via* preparative column chromatography contains only trace quantities of the two curcuminoids (see Fig. 3b and Table 2). On the other hand, for the case of the other two curcuminoids, DMC and BDMC, obtaining a pristine surface of these curcuminoids seems to be a practically difficult task as TOF-SIMS results confirmed that both of these samples contain significant amounts of impurities. It should be mentioned here that the HPLC analysis confirmed that the curcuminoids DMC and BDMC are pristine materials (see Table 2). In particular, HPLC confirmed that the sample DMC_s contains only trace quantities of CUR as opposed to the 23 wt% of CUR determined using the TOF-SIMS technique. This observation does not limit the usefulness of the TOF-SIMS technique. Rather it is a useful finding, and it exposes the sensitivity of this technique. TOF-SIMS detects even the presence of impurities in trace amounts on the surface under focus. For instance, the molecular ion peak $[M + H]^+$ of CUR, BDMC, and DMC alone is enough to simultaneously quantify the weight percentage of impurities and to identify the location of impurities on the crystal surface.

The high sensitivity of this technique can also be imaged *via* obtaining a chemical map of the individual components and determining how they are distributed on the surface. Fig. 4 shows the colored ion images of the characteristic molecular ion peaks of CUR, BDMC and DMC and the RGB (red for CUR, green for DMC and blue for BDMC) overlay image of all the three reference samples, Cur_s (Fig. 4a), DMC_s (Fig. 4b) and BDMC_s (Fig. 4c). TOF-SIMS clearly produced well-defined images that are specific to intact individual molecular components. The overlay image shows that very little overlap is seen on the reference compounds and this should allow us to locate the concentration or the distribution of these compounds on the sample surface. The overlay images clearly show pure red, green and blue colours that correspond to CUR, DMC and BDMC, in the curcuminoid standards, CUR_s, DMC_s and BDMC_s, respectively. Clearly the colored ion images of the molecular ions specific to the curcuminoid molecules and their RGB overlay can expose the distribution of these molecules on the surface. These chemical images, while clearly exposing the

near pristine nature of each of the pure components, also provide the map of the other impurities (or components) that are present in trace quantities (that cannot be detected using the conventional HPLC technique) in each of these pure curcuminoid standards.

3.4. Positive ion TOF-SIMS spectrum of the crude curcumin

To test the sensitivity of TOF-SIMS to identify the percentage composition and the quality of the starting crude solid product in terms of purity, the surface of the crude curcumin was chemically mapped to identify the target molecule curcumin and the two other structurally similar impurities. The positive ion TOF-SIMS spectrum of the crude curcumin shown in Fig. S2 of the ESI† contains several major peaks that include the molecular ions of the intact CUR, DMC and BDMC and several other peaks which correspond to other fragment ions of these individual components shown earlier in Fig. 3a. For convenience, in Fig. 5a, we plotted only the three major peaks (m/z 309, m/z 339 and m/z 369) that correspond to the intact curcuminoids. From the peak intensity (and the peak area), it can be realised that CUR is the major component in the crude curcumin, followed by DMC and BDMC.

The curcuminoids CUR, DMC and BDMC have similar molecular weight and if we assume that the ionization probability is the same, then the sum of the areas of the peaks of each component must be proportional to the total concentration of these components altogether. Thus, from the peak area, it is possible to obtain quantitative information about the product purity. To test the validity of this assumption, in Fig. 5b we plotted the chemical composition of the crude curcumin calculated based on the area of the molecular ion peak of CUR, DMC and BDMC. According to the peak area, the crude composition was estimated to be BDMC: 9.56 wt%, DMC: 24.06 wt% and CUR: 66.38 wt% (see Table 2). These values differ from the HPLC determined values given by CUR: 78.6 wt%, DMC: 17.7 wt%, and BDMC: 3.6 wt% (see Table 2). Clearly the concentration determined by HPLC and TOF-SIMS differs. The quantitative relationship between HPLC results and the ones obtained from the molecular ion peaks is difficult to obtain due to the complexity associated with the ionization mechanism or also called the matrix effect.[17,37] It should be remembered that the resolution of these techniques and their working principles are different. It is possible to obtain a clear separation of the individual components with chromatographic techniques and their percentage composition in the bulk of the material can be quantified. On the other hand, in static mode, TOF-SIMS can only recognize the chemical composition on the top surface layer of atoms or molecules.[38] If the surface under inspection contains more than one component (in our case, the surface contains CUR, DMC and BDMC), the ionization probability is changed by the interaction of more than two types of materials or also called as the matrix effect. In that case, the
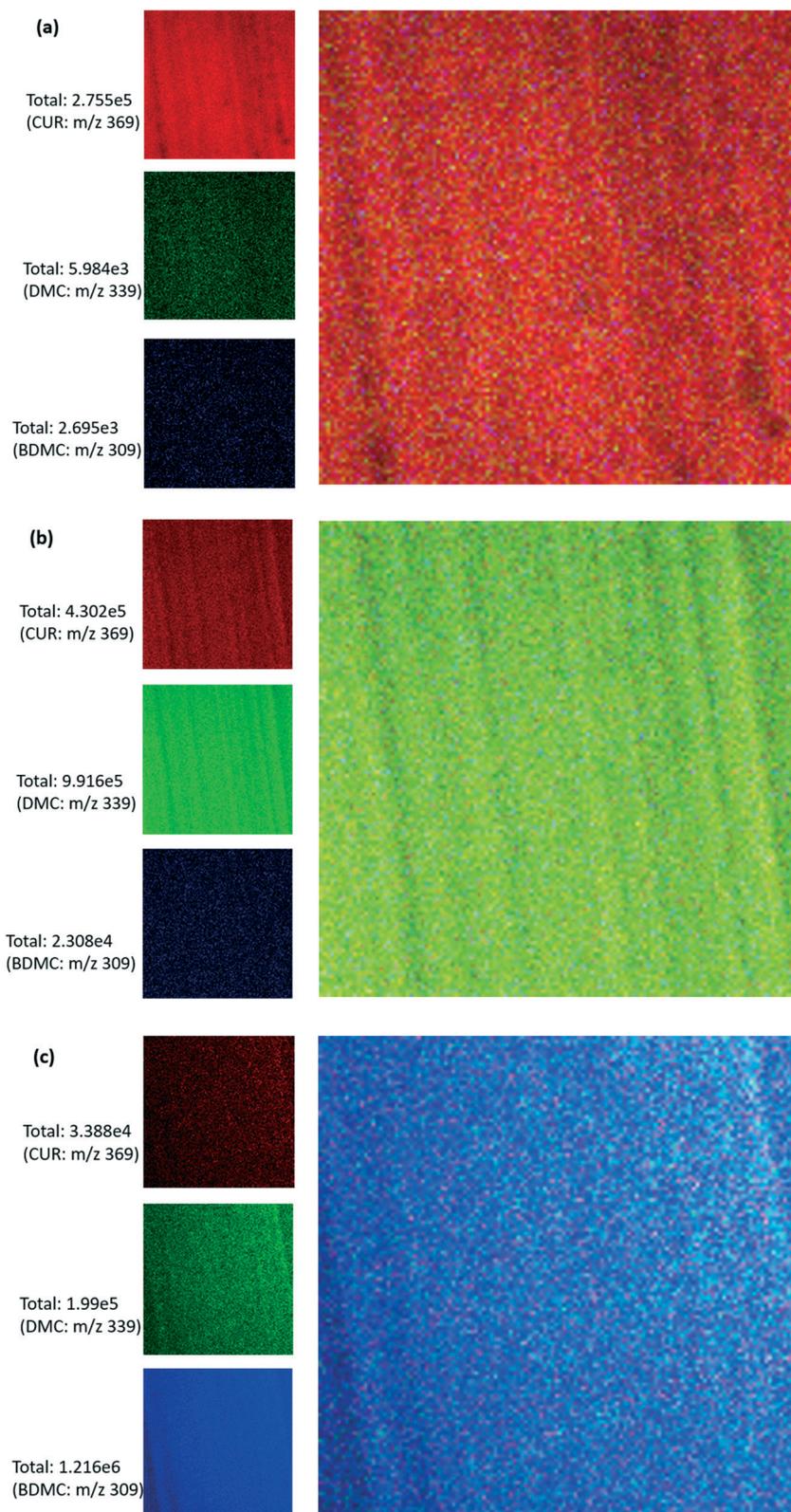
Fig. 4 Colored TOF-SIMS maps of the secondary positive ions of CUR (m/z 369), DMC (m/z 339) and BDMC (m/z 309) in the curcuminoid standards, (a) CUR_s, (b) DMC_s and (c) BDMC_s. Top, middle and bottom rows in the left panel of each image correspond to the chemical map of CUR (m/z 369), DMC (m/z 339) and BDMC (m/z 309) and their RGB overlay is shown on the right panel (CUR: red, DMC: green and BDMC: blue). Note: brighter colour corresponds to higher concentration of the specific ion (m/z). The RGB overlay shows that the curcuminoid standards are essentially pure and the ion images clearly indicate that the curcuminoids are evenly distributed. The field of view of analysis is 300 × 300 μm². In the figure and also throughout the manuscript, together with the positive ion images, we also provided the yield of each curcuminoid (positive) ions for reference purposes.
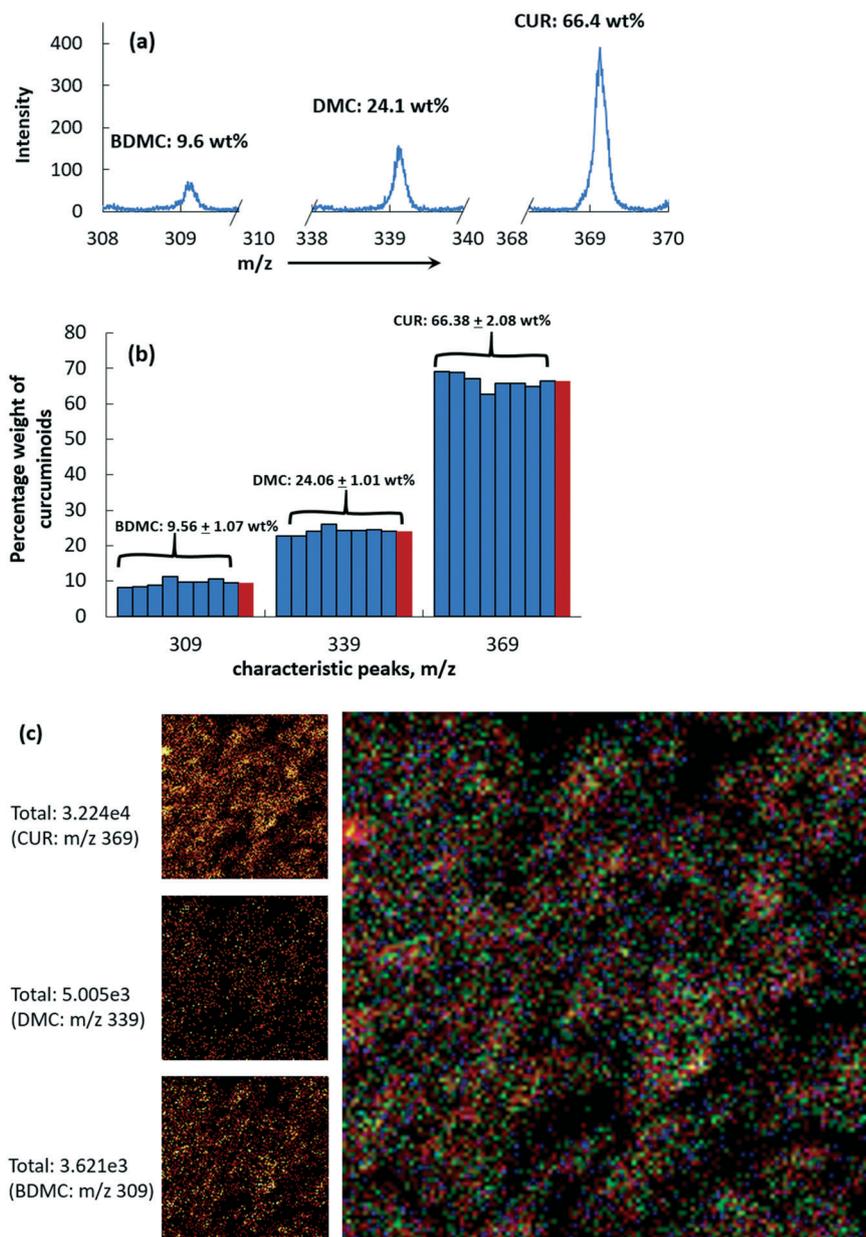
Fig. 5 (a) The major signals that correspond to the intact molecules of CUR, DMC, and BDMC in the positive ion TOF-SIMS spectrum obtained from a sample spot of the solid crude curcumin samples. The weight percentage of the curcuminoids was calculated from their peak area. (b) The weight percentage (and their standard deviations) of the curcuminoids measured in the crude curcumin. Note: the percentage weight of the curcuminoids shown in figure (red bars) corresponds to the average of the area of the molecular ion peaks obtained in spectroscopy mode at four different spots per sample across two samples. The blue bars correspond to the peak area of the curcuminoids obtained from each spot. (c) Left panel: Secondary positive ion images of CUR (m/z 369), DMC (m/z 339) and BDMC (m/z 309) in the crude curcumin. Right panel: The RGB (red: CUR, green: DMC and blue: BDMC) overlay of the curcuminoids in the crude CUR. Note: brighter colour corresponds to higher concentration of the specific ion (m/z). RGB overlay shows that both DMC and BDMC are evenly distributed in the pulverised sample. The field of view of analysis is $300 \times 300 \ \mu m^2$.

ratio of the absolute TOF-SIMS counts for the three compounds can be different than the actual concentration of these materials as the ionization probability depends on the material itself. The predicted weight percentage of CUR based on the area of the molecular ion peak was slightly lower than the values obtained from HPLC. This seems to be a common observation while using the TOF-SIMS technique to predict the concentration of the molecules as the ionization probability or the efficiency of ionization and ion yield depends on the type of the molecule and the environment.[37] In a few cases, the ionization probability of the material can lead to lower counts for the higher concentration material.[23,37,39] Another issue in quantifying the impurity concentration on the surface is that the relationship between

the peak area ratios of impurity to CUR *versus* the impurity concentration does not necessarily need to be linear.[37] In the present case, the as-received crude curcumin from the supplier was a fully pulverised and homogeneous mixture that contains all the three curcuminoids. Thus, we expect that the surface concentration of CUR and the impurities should reflect the characteristic weight percentage of these compounds in the bulk of the sample and may match with the values determined using the HPLC technique. The peak intensity will also be influenced by the concentration of impurities on the surface. If the impurities are present in lower concentration, at sub-monolayer coverage, then typically there exists a linear relationship between the selected ion peak intensity and the concentration of the compound of interest. At higher concentrations, there can exist a non-linear relationship between the peak intensity/ peak area (as in the present case) and the concentration of the impurities and quantification of impurity concentration merely based on the peak area will be complex. Our experimental results show that, for the case of solid curcumin samples, it may not be a straightforward approach to determine the percentage impurity on the surface merely based on the ion counts of each component. Nevertheless, if we compare the composition of curcuminoids obtained from HPLC and TOF-SIMS (see Table 2), it can be realised that the global trend is not influenced by the above discussed matrix effect. Both TOF-SIMS and HPLC confirm that the crude material contains a higher amount of CUR, followed by DMC and BDMC. The higher the composition of CUR in the sample as determined by HPLC, the higher the area of the molecular ion peak of CUR in the TOF-SIMS spectra.

Despite the results obtained from TOF-SIMS being biased due to the matrix effect and thus cannot be matched to the ones obtained from HPLC, both techniques should complement each other while characterising solid materials. For instance, HPLC can provide the bulk composition, whereas TOF-SIMS can give quantitative information about the composition of curcuminoids on the surface under the analysis window. It is worth mentioning here that the above discussed limitation (matrix effect) can be possibly mitigated by preparing thin films of the bulk product which that can be made by drop casting or spin coating of a highly diluted solution of the crude curcumin in a suitable substrate. This way it is possible to evenly deposit a few layers of the targeted compounds on the substrate surface (similar to the experimental protocol used to collect the reference spectra – see section 2.2.). This is not performed in this study for the crude curcumin because the main focus here is to obtain a chemical map of the surface rather than the bulk of the material. In any case, these limitations or the requirement for a rigorous experimental protocol do not limit the usefulness of this method which is to spatially resolve the chemical data. In Fig. 5c we showed the molecular ion images of CUR, DMC and BDMC in the crude curcumin; also shown is the RGB overlay of these components. Clearly, the TOF-SIMS images show that both the structurally similar

impurities, DMC and BDMC, are homogenously distributed which can be expected from a completely pulverized product. The molecular ion images shown in Fig. 5c are obtained in spectroscopy mode and if required the image resolution can be improved by acquiring the ion images in imaging mode (this issue is discussed in detail in the later section).

3.5. TOF-SIMS characterization of the crystals obtained from cooling crystallization experiments

Fig. 6 shows the percentage composition of the curcuminoids on the surface of CUR_n, CUR_n_impure, and CUR_sph. As mentioned earlier, the percentage composition was determined based on the peak area of their molecular ions. Clearly the concentration determined by HPLC (see Table 2) and TOF-SIMS does not produce similar results. There is a global trend between the HPLC results and the ones obtained from the molecular ion peaks (see Table 2); the higher the concentration of CUR, the higher the ion counts for this compound in the bulk of the sample. One noteworthy observation is that TOF-SIMS detects a significant amount of impurities (roughly 10%) in five-time recrystallized sample (CUR_n, see Fig. 6a) which contains impurities only in trace amounts as confirmed by HPLC. We observed this trend also in Cur_n_impure (see Fig. 6b) that contains roughly 92 wt% of DMC and no BDMC (see the values determined by HPLC in Table 2). TOF-SIMS predicts a slightly larger value for DMC (~75 wt% *versus* 92 wt% from HPLC) and BDMC (3.74 wt% from TOF-SIMS *versus* a negligible amount from HPLC). For the case of spherulites, TOF-SIMS predicted values significantly vary with the ones obtained from HPLC. It is worth mentioning here that, while analysing the spherulites using TOF-SIMS, the spherulites were gently crushed while depositing them on the sticky tape before analysis. The curcumin spherulites are roughly 80 microns (see Fig. 2g–i) and made up of several small nanometre sized crystallites (roughly 20 nm thick and 500 nm long) and thus the final structure exhibits a crystallographic hierarchy. These small crystallites are aggregated but spatially-separated exhibiting the properties of the mesocrystals. As TOF-SIMS is a surface technique and we intend to identify the location of the impurities in the crystallites, we crushed the spherulite gently without pulverising the samples and then we placed it on the sample stage. Crushing the spherulites gently separates the loosely aggregated crystallites, helps to cleave the spherulite structure and can expose the core of spherulite to the ion beam. Additionally, we crushed the spherulites to observe the concentration of the curcuminoids on the surface of the nanocrystallites that are spatially separated in the spherulites. Furthermore, in the case of spherulites, the intensity of the ion peaks will also be diminished due to the particle topology, especially during imaging. The spherical nature of the product will affect the resolution due to distortion, shadowing, and field effects and let's not to forget that the ion yield also depends on the incidence angle of the primary ion beam.[14] Unless the spherulites are crushed, most
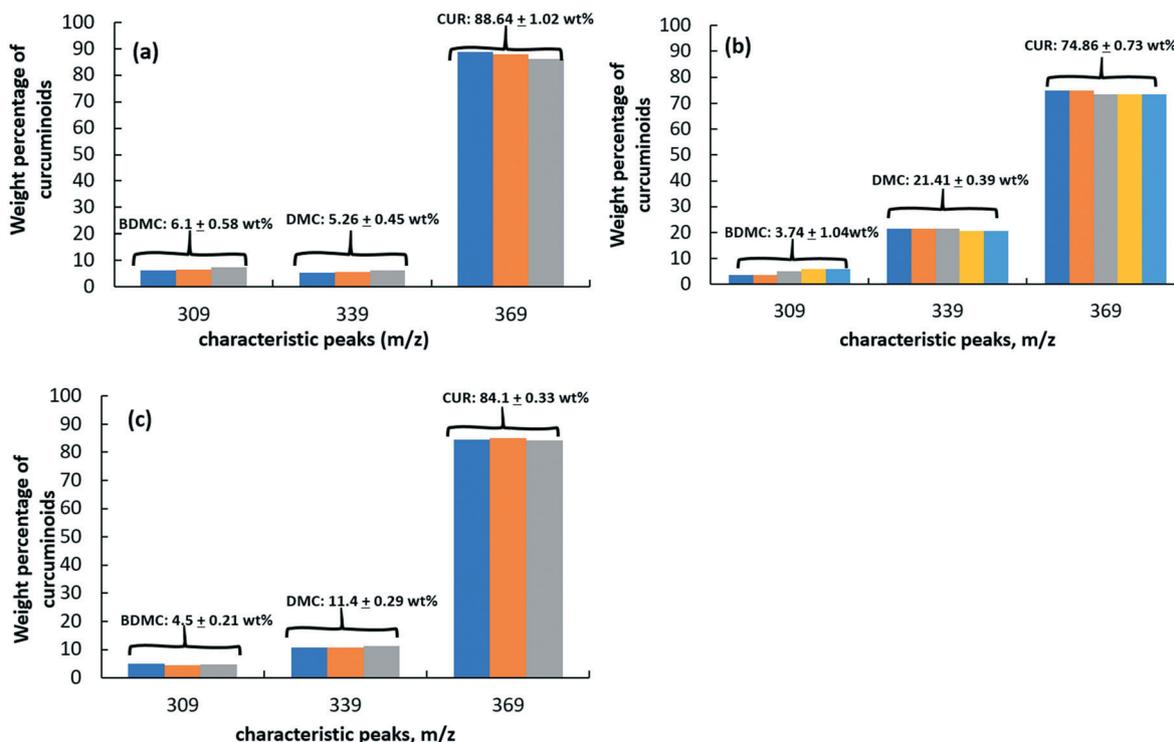
Fig. 6 Percentage weight of the curcuminoids (BDMC, DMC and CUR) in (a) five-time recrystallised curcumin, CUR_n, (b) one time recrystallised curcumin of nominal purity, CUR_n_impure, and (c) curcumin spherulites, CUR_sph.

of the information on the composition of the different components in the unit mass of the spherulites or the bulk volume will be massively blurred. For the case of crushed spherulites, as the samples are crushed rather than using the full spherulite structure, it should give the percentage composition of the curcuminoids comparable to the bulk of the product obtained with the HPLC technique. It can be observed from Fig. 6 that the TOF-SIMS obtained values vary significantly with the HPLC obtained values. For instance, according to HPLC, spherulites contain no BDMC and trace quantities of DMC. On the other hand, TOF-SIMS detects up to 10 wt% of impurities (3.74 wt% BDMC and 9.22 wt% DMC). These values match with the TOF-SIMS determined impurity concentrations in the five-time recrystallized sample (CUR_n), which is supposedly a pure curcumin as confirmed by HPLC. These discrepancies in the results obtained from HPLC and TOF-SIMS can be explained based on the working principles of TOF-SIMS. If the primary ions bombard the surface and produced a molecular fragment of atomic mass unit similar to that of the molecular ions of DMC or BDMC, then it is possible to expect a slightly higher concentration of these units on the surface of the sample. This effect will also alter the local environment, and this will alter both the ionisation efficiency and the yield of ions with respect to the impurities, DMC and BDMC.

The ionisation efficiency and yields of ions will contribute to the changes with respect to the species and the local environment. TOF-SIMS is sensitive to almost the first molecular monolayer of a sample within the static

operational regime (book) and it is more likely that, the recorded DMC and BDMC could be the deposits of the impurities on the surface of the crystallites from the mother liquor that contains a significant amount of impurities. In any case, we eliminated this possibility by rinsing all the samples with an isopropanol/water (70/30 v/v) solvent mixture at least ten times to ensure that the surfaces are free of the mother liquor. It should be stressed here that TOF-SIMS is not essentially a technique suitable to predict the bulk properties, and the SIMS spectra cannot be simply compared to the ones obtained from conventional spectroscopic/chromatographic techniques. TOF-SIMS relies on the degree of ionization and involves disruption of molecules during the measurement and thus cannot be easily correlated to the values obtained from HPLC techniques where the analyte molecules are kept intact. The interaction of energetic ions with solid samples of organic compounds could create a complex sequence of phenomena and thus the link between the initial conditions and the final SIMS spectra may be often different. In the present study, this issue can be realized from the percentage composition of the curcuminoids in CUR_n which is supposedly a pristine material with only trace quantities of impurities. One reason can be attributed to the fundamental aspects of the interaction between energetic ions and the surface of the organic materials. The level of damage induced by primary ions, extent of molecular fragmentation, rearrangement and chemical reactions induced by primary ions on solid samples all can influence on the SIMS spectra.[14] The discrepancy in the weight

percentage of the curcuminoids determined using HPLC and TOF-SIMS can also be attributed to the crystallisation mechanism itself. During the cooling crystallisation, at the early stage of the nucleation, the target molecules tend to assemble to form prenucleation clusters which may evolve into stable crystallites or also called stable nuclei. These nuclei can be essentially pure, however, during the growth of these nuclei, it is more likely that the impurities may adsorb or replace the crystal lattice. The impurity transfer can take place, at the later stage of the crystallisation, when the supersaturation approaches the solubility concentration. In that case, only the external surface of the crystals will contain impurities. The concentration of the impurity on the surface of the crystals may be of negligible quantity when compared to the concentration of the entire bulk crystal of curcumin. As TOF-SIMS characterise very few layers on the surface of the crystals, it cannot represent the bulk properties of the crystals characterised using HPLC.

To check the limitation of the TOF-SIMS technique, we prepared a dilute solution of CUR_sph and CUR_n using isopropanol as a solvent followed by dip coating of this solution on aluminium foil. Fig. 7a and b show the molecular ion peaks $[M + H]^+$ of CUR, BDMC, and DMC in the surface dip coated with the solutions of CUR_sph and CUR_n, respectively. For comparison purposes, in these figures, we also showed the molecular ion peaks $[M + H]^+$ of the intact curcuminoids obtained from their solid crystalline materials. Based on the area of these peaks, we calculated the weight percentage of the curcuminoids in these samples. The TOF-SIMS spectra from the Al foil coated with these solutions show that CUR_s contains 0.36 wt% BDMC and 1.74 wt% DMC and CUR_n contains 0.32 wt% of BDMC and 1.45 wt% of DMC. These values indicate that these samples are essentially pure which agrees with the results obtained using the HPLC technique (see Table 2). However, these values do not match with the weight percentage of the impurities obtained directly from the solid crystalline materials using TOF-SIMS (see Fig. 6a and c). Clearly, the sample preparation technique itself plays a big role in the sensitivity of the TOF-SIMS technique. In the case of solid samples, deposited on sticky-tape (see section 2.4.), the surface is clearly not a flat surface. In this case, the primary ion projectile could hit different faces of the crystal and thus the chemical environment within the raster area would be completely different to that of the dip coated surfaces. Typically, the primary ions penetrating the solid surface will cause successive collisions with atoms and molecules, transferring energies producing different molecular fragments, and can produce SIMS spectra that may differ from the characteristic property of the actual target molecules.[14]

In Fig. 8a and b, we show the colored ion images of the characteristic molecular ion peaks of CUR, DMC and BDMC and the RGB (red for CUR, green for DMC and blue for BDMC) overlay image of solid samples of CUR_sph and their solution coated on the Al foil, respectively. In the case of the CUR_s sample prepared using the dip coating technique, the overlay image clearly shows red colour that corresponds to CUR. This means that the CUR_s sample is essentially pure. On the other hand, the RGB overlay of the solid samples of CUR_s shows the distribution of red, green and blue colours on the samples. This clearly indicates that the impurities are distributed evenly and slightly in higher concentration (when compared to the same sample prepared *via* dip coating) on the surface of the crystallites.

Likewise, we observed such discrepancies in the positive ion peak area of the curcuminoids in the as-crystallised
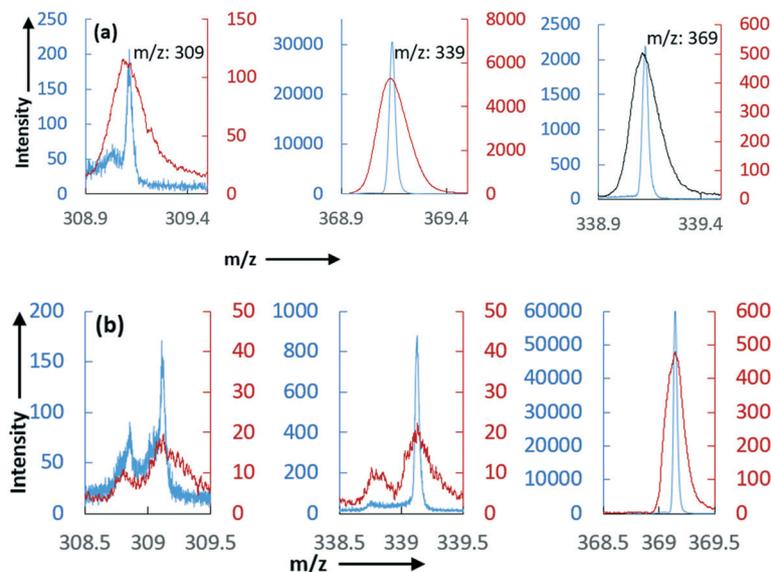

Fig. 7 The major signals that correspond to the intact molecules of CUR, DMC, and BDMC in the positive ion TOF–SIMS spectrum obtained from a sample spot on the surface of (a) CUR_s and (b) CUR_n. The weight percentage of the curcuminoids in the drop cast samples shown in the figure was obtained from their peak area.
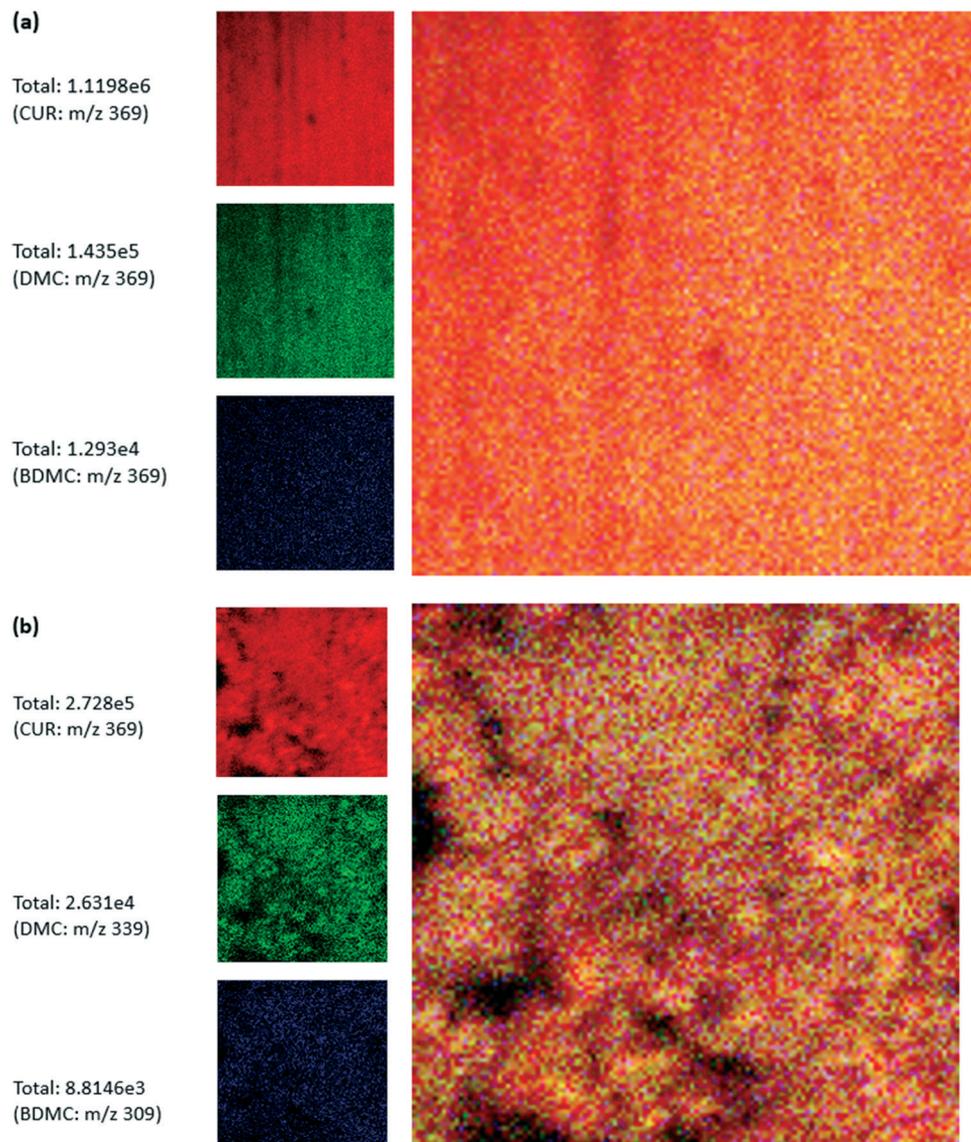
Fig. 8 Coloured TOF-SIMS ion maps (field of view: $300 \times 300~\mu m^2$) of CUR, DMC and BDMC in the (a) surface of the aluminium foil coated with a solution of curcumin spherulites and (b) the surface of the solid curcumin spherulites. The field of view of analysis is $300 \times 300~\mu m^2$.

CUR_n sample (Fig. 9a) and the same sample prepared *via* dip coating (Fig. 9b). If we compare the RGB overlay images in Fig. 9a and b, it can be realised that the sample preparation method influences the experimental outcome. The RGB overlay of the CUR_n sample prepared using the dip coating technique shows red colour that corresponds to CUR. In the RGB overlay of the solid samples of CUR_n, although the sample predominantly contains CUR, we observed a uniform distribution of green and blue colours on the surface of the samples that correspond to DMC and BDMC. This clearly indicates that the impurities are distributed evenly on the surface of the curcumin crystals and in concentration slightly higher than the ones observed on the dip coated surface. It should be remembered that the degree of molecular fragmentation will be different depending on the crystal face under the beam of the primary

ions. For instance, the methoxy groups are more vulnerable if the primary ions impinge on the (1 0 0) face (see Fig. 10a). Likewise, the projectile of the primary ions hitting on the (0 1 0) plane (see Fig. 10b) can bombard 80% of the CUR structure plus the methoxy and hydroxyl groups attached to one end of the aromatic ring. In the (0 0 1) (see Fig. 10c) plane, the hydroxyl group and the keto-oxygen are vulnerable to the primary ions. These effects can be minimized by preparing a homogenous surface *via* solution drop-casting techniques as used in this work to obtain the reference spectra of curcuminoids.

Finally, we also obtained the chemical map of the CUR_n_impure crystals using TOF-SIMs in spectroscopy mode (see Fig. 11). For convenience, together with the RGB overlay, we show the chemical maps of different ions, CUR, DMC and BDMC in red, blue and green, respectively. Within
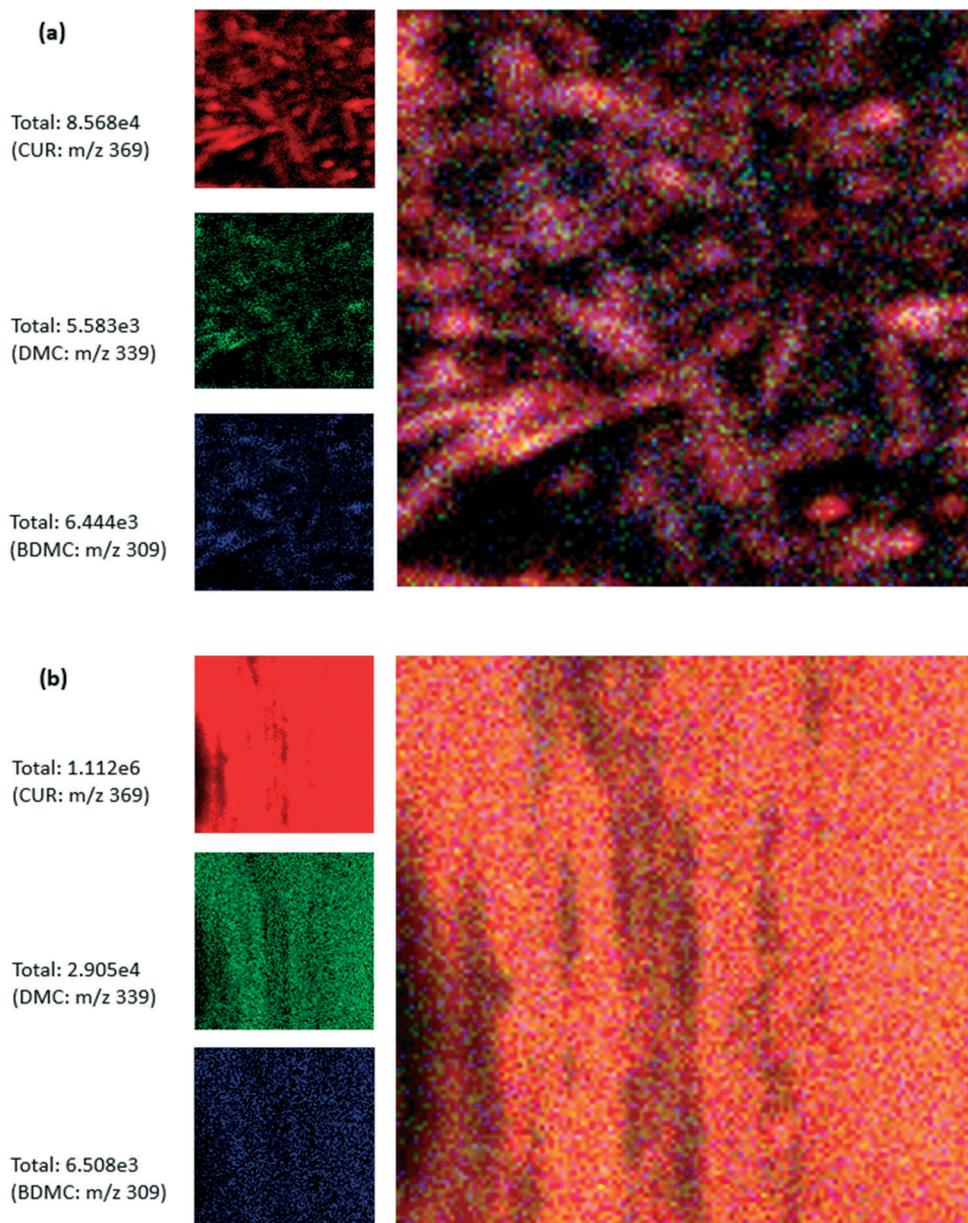
Fig. 9 Coloured TOF-SIMS maps of positive ions of CUR, DMC and BDMC in (a) the surface of the five time recrystallised curcumin, CUR_n, and (b) the surface of the aluminium foil coated with a solution of the five time recrystallised curcumin. The field of view of analysis is $300 \times 300\ \mu m^2$.

the field of view of analysis, we have roughly seven to eight crystals. The coloured ion maps clearly show that the impurities are evenly distributed on the surfaces of these crystals. There are several locations where we observed green
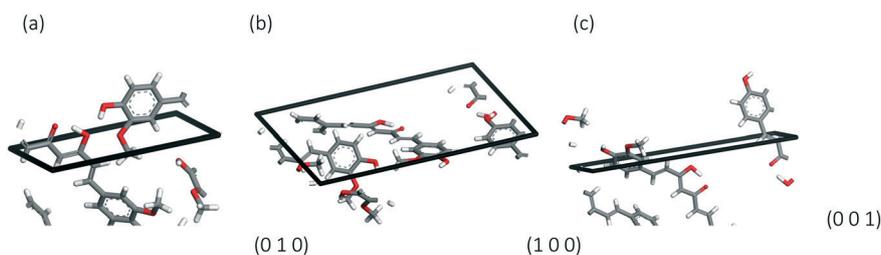

Fig. 10 The types of functional groups on different crystal planes which are exposed to the primary ions, (a) (0 0 1) face, (b) (0 1 0) face and (c) (1 0 0) face. The crystal facets are cleaved from their crystallographic structure (of FI curcumin).
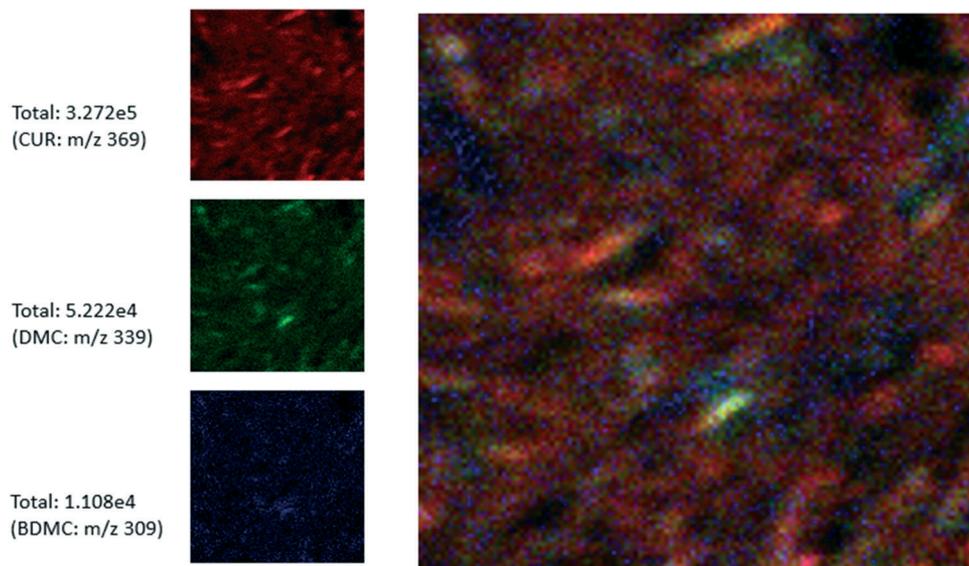
Fig. 11 Coloured TOF-SIMS maps of positive ions of CUR, DMC and BDMC in the surface of the one-time recrystallised curcumin from its crude product, CUR_n_impure. The field of view of analysis is 300 × 300 μm².

and blue spots on the surface of the crystals within the field of view of analysis. This clearly indicates that the impurities are evenly distributed and occupy their own site on the crystal surface. We also observed a brighter green spot on the crystal. This means that the concentration of one of the structurally similar impurities is relatively higher in that crystal when compared to other crystals in the sample. Another notable observation is that the overlay image contains new colours, which indicates that the two structurally-similar impurities adsorb on the same site. This is crucial information from the crystal growth science viewpoint as it clearly indicates that all the facets of the crystal show equal affinity towards the two structurally similar impurities. Additionally, a site which can preferentially adsorb or replace DMC can also host or replace BDMC during the crystallisation process. This can be expected, as the impurities are structurally similar to the crystallising compound (CUR) and in that case, during nucleation and crystal growth, these impurities DMC and BDMC can incorporate into the crystal *via* lattice replacement.

3.6. TOF-SIMS characterization of the crystals obtained from the crystal growth experiment

Fig. 12a shows the weight percentage of the curcuminoids on the surface of the Cur_cg crystals. To improve the statistics, we obtained the TOF-SIMS results at three different spots (the field of view of analysis in each spot is 300 × 300 μm²), all in spectroscopy mode. It is clear from Fig. 12a that the weight percentage of the curcuminoids is the same in all the three spots, which clearly indicates that the impurities are evenly distributed in the bulk sample. The surface contains both structurally similar impurities, ~4% of BDMC and ~21% DMC. This clearly indicates that the impurities are

incorporated into the crystals during the crystal growth process. It is worth mentioning here that the surface composition as well as the distribution of curcuminoids of the pure crystals grown in an impure solution (CUR_cg) is comparable to the surface composition of the curcuminoids in the crystals obtained from one-time recrystallisation experiments (CUR_n_impure, see Fig. 6b). Despite the fact that the cooling crystallisation and the slow-evaporation crystal growth experiments are performed using different experimental protocols, the TOF-SIMS results clearly indicate that impurities are transferred into the solids during the crystal growth process. In terms of the location of impurities, the ion images acquired in spectroscopy mode (see Fig. 12b) clearly indicate that, within the field of view of analysis, the impurities are evenly distributed on the surface of all the crystals. The coloured ion maps clearly show that DMC and BDMC are evenly distributed on the crystal surface. Additionally, the presence of new colours plus clearly blue and green spots on the crystal surface indicates that DMC and BDMC either evenly occupy individual sites on the crystal surface or both impurities occupy the same site on the crystal surface. It is worth mentioning here that the TOF-SIMS results obtained for the CUR_cg sample cannot be compared with the ones obtained from HPLC as we started the crystal growth experiment with pristine crystals that contain only CUR, and we expect that the impurities are transferred onto the surface of crystals *via* adsorption or *via* lattice replacement during the growth process either at one crystal face or all the crystal facets. Thus, the properties of the bulk crystal will differ from the surface composition. The ion images clearly show that the impurities are distributed evenly on the surface of the all the crystal facets observed within the analysis window.

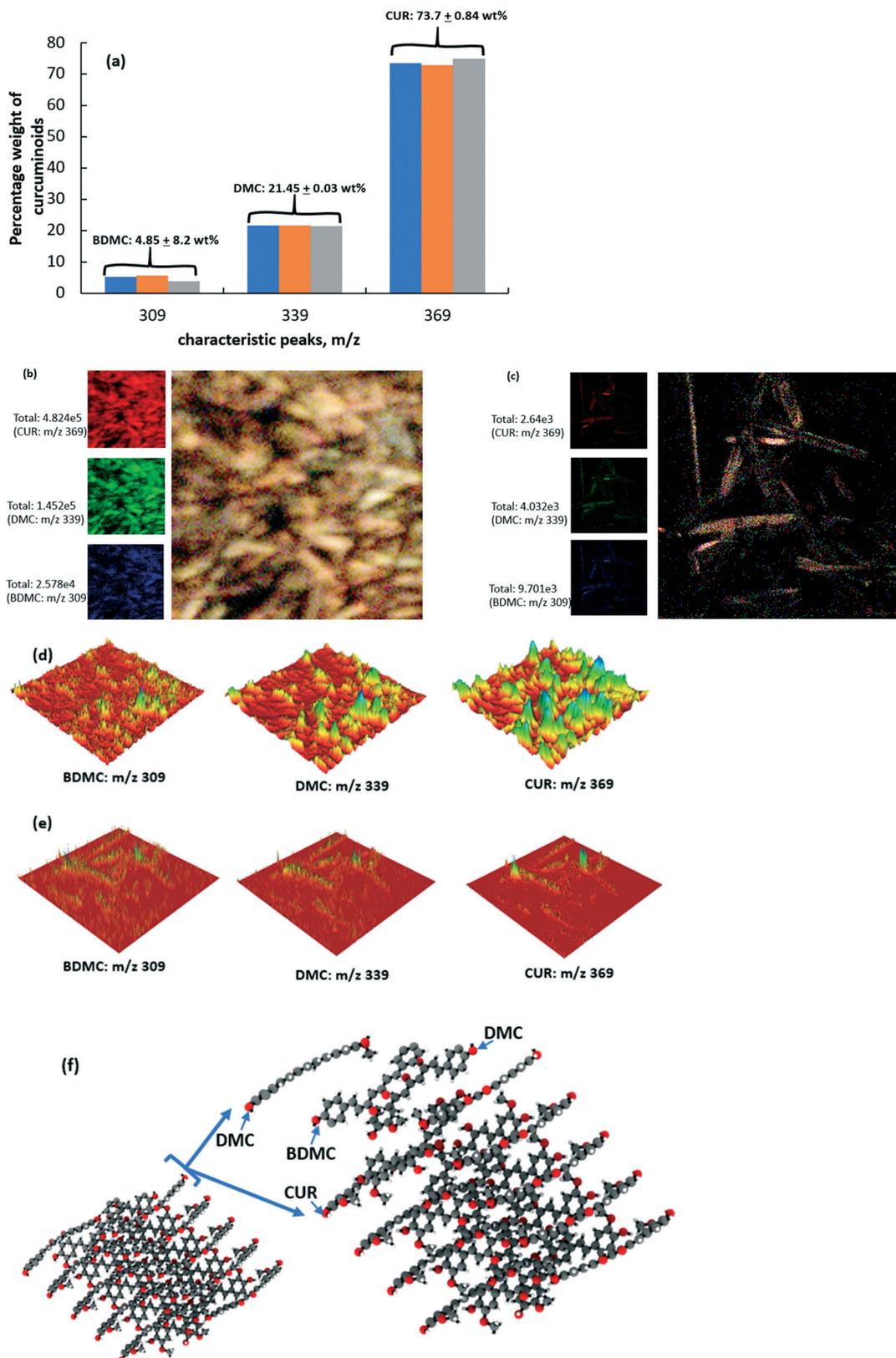So far, we discussed all the results based on the TOF-SIMS spectra and the positive ion images obtained in the

Fig. 12 (a) Percentage weight of the curcuminoids (BDMC, DMC and CUR) in the surface of the crystals obtained from the crystal growth experiment (CUR_cg), (b) coloured TOF-SIMS ion maps (field of view: $300 \times 300 \ \mu m^2$) of CUR, DMC and BDMC in the surface of CUR_cg, (c) (b) coloured TOF-SIMS ion maps (field of view: $130 \times 130 \ \mu m^2$) of CUR, DMC and BDMC in the surface of CUR_cg, (d) carpet map showing the locations and yield of positive ions of the curcuminoids obtained in spectroscopy mode (field of view: $300 \times 300 \ \mu m^2$), (e) carpet map reflecting the yield of curcuminoid positive ions and their locations in imaging mode (field of view: $130 \times 130 \ \mu m^2$), and (f) a model surface of the solid curcumin crystals, where the curcumin molecules are replaced by DMC and BDMC in the lattice (lattice not shown).

spectroscopy mode. Except for spherulites and the crude curcumin, all the other samples obtained from cooling crystallisation and crystal growth experiments produced needle shaped crystals. These crystals are roughly around 180–200 μm by length and 20–30 μm by width and there exists a size distribution in the final samples. In this work for the spectroscopy mode, we set the field of view of analysis to 300×300 μm^2 and while imaging, we set the field of view of analysis to 130×130 μm^2. As we mentioned earlier, primary ions generate a damage front ahead of the sputtering regime; this means that the molecular ions and fragment ions obtained represent only the outermost layer of the sample. This in turn alters the total ion yield depending on the spatial resolution. The higher the spatial resolution, the lower the number of molecules in the area of a single pixel and the number of ions that can be generated and detected from the area will decrease proportionally with the spatial resolution. In spectroscopy mode, the analysis window which we set is sufficient to characterise roughly up to fifteen to twenty crystals and the ion yield is sufficient to characterise the weight percentage of curcuminoids on the surface under the field of view of analysis. Thus, the positive ion spectra collected over three to five different spots per sample should provide characteristic and quantitative information about the distribution and location of the curcuminoids on the surfaces of the crystals. In imaging mode, despite the fact the set analysis window can roughly expose the weight percentage of the curcuminoids on the surface of crystal facets, it compromised the total ion yield, making it difficult to quantify the weigh percentage of the curcuminoids on the sample. On the other hand, the imaging mode provides a better image resolution which allows us to observe the distribution of impurities on the crystal facets. For comparison purposes, in Fig. 12b and c, we showed the coloured ion maps of the three curcuminoids and the RGB overlay in CUR_cg obtained in spectroscopy and imaging mode, respectively. The coloured ion maps in Fig. 12b and c clearly indicate that the impurities are evenly distributed on the crystal surface. The images acquired in imaging model provide a better magnification of the location of impurities on the crystal facets. The crystals are essentially needle shaped with a high aspect ratio and this makes it difficult to focus on a particular facet of the curcumin crystals. However, in the imaging mode, within the field of view of analysis, it is possible to recognize that all the facets contain the two structurally similar impurities, and they are evenly distributed (see the coloured ion maps of DMC and BDMC shown in Fig. 12c). Another notable observation is that the RGB overlay image in Fig. 12c contains several secondary colours. This indicates that the curcuminoids are located on the same area of the surface. This can occur when the topmost few layers of the surface are formed by the ordered arrangement of the curcuminoids on top of each other. This indicates that, the structurally similar impurities BDMC and DMC should have replaced the curcumin molecules in the crystal lattice (see Fig. 12f where we showed a model

representation of the curcumin molecules in the crystal lattice replaced by the structurally similar impurities BDMC and DMC). In Fig. 12d and e, we represented the ion images of the curcuminoids obtained in spectroscopy and imaging modes in the form of a carpet plot, respectively. The higher the number of peaks and the higher the peak heights on the carpet plot, the higher the ion yield with respect to that of the molecular ion on the surface. Clearly, the ion yield is better in spectroscopic mode, which is required to obtain quantitative information about the surface composition. Additionally, the carpet plot of the ion images obtained in spectroscopy mode clearly shows that the impurities are evenly distributed on the surface of the crystals under the field of view. Experimentally, irrespective of the mode of operation, the statistics can be improved by acquiring the TOF-SIMS spectra or the ion images at multiple locations over multiple samples.

4. Summary and conclusions

Impurities are unavoidable and are frequently encountered during the crystallisation of several active pharmaceutical ingredients. To date, the effect of impurities is often studied using theoretical models which mostly rely on the concept of impurity adsorption or impurity incorporation into the crystals *via* lattice replacement. The effect of impurities can be better understood, if we have information on the location of the impurities during the crystallisation process. In this work, we successfully used TOF-SIMS to determine the composition of the two different but structurally similar impurities, DMC and BDMC plus their locations on the surface of crystals of the target compound, CUR. We showed that the surface of curcumin crystals obtained from cooling crystallisation and crystal growth experiments is enriched with structurally similar impurities and more importantly, they are homogeneously distributed. Additionally, we discussed the limitations of this technique and how the ion yield of each curcuminoid is altered by the sample preparation method.

TOF-SIMS is a very useful technique and if the samples are carefully prepared, it can provide quantitative to semi-quantitative information about the concentration of the impurities and can easily spot the location of the impurities on the crystal surfaces. If used with other analytical techniques like HPLC, TOF-SMS can help to simultaneously quantify both the surface concentration of the impurities and their locations on the crystal facets. As we showed in this work, the chemical properties of bulk crystals can be characterised at the molecular level by probing the surface coated with the dilute solution of the bulk crystals using TOF-SIMS. Another key finding from this work is that the TOF-SIMS ion maps provided new evidence which reveals that the structurally similar impurities occupy either different sites or the same sites on the surface of all the crystal facets. The latter can be attributed to the replacement of the crystal lattice by both impurities. This information is useful from

the crystal growth viewpoint. The effect of impurities on the crystal growth process is often discussed based on the impurity pinning mechanisms. At least for the studied systems, it is more likely that the crystal growth may still proceed even after the attachment of structurally similar impurities on the kink sites, as here the impurities merely replace the curcumin molecule instead of pinning the growth steps (this should be tested through separate crystal growth kinetic experiments, which is beyond the scope of this work). The results obtained from TOF-SIMS can even be used to gain understanding on the nucleation mechanism. For instance, Heffernan *et al.*[1] studied the nucleation kinetics of the curcumin in the presence of structurally similar impurities, DMC and BDMC, and they found that these impurities decrease the nucleation rate. They also theoretically showed that the decrease in the nucleation rate in the presence of these impurities was associated with a noticeable decrease in the pre-exponential factor and a negligible change in the surface energy. In this work TOF-SIMS ion images clearly suggest that impurities are incorporated into crystals possibly *via* lattice replacement as the curcuminoids seem to occupy the same spot at multiple locations on the crystal surface. As crystallisation is an inherently multi-scale process, it is reasonable to assume that the bulk properties of the crystal reflect the properties of solid structures formed *via* nucleation and even the pre-nucleation clusters. Based on the findings obtained from TOF-SIMS, it is possible to theoretically propose that the incorporation of structurally-similar impurities *via* lattice replacement may not alter the surface energy (thermodynamic factor associated with crystallisation), but can alter the (kinetic) pre-exponential factor. Similarly, TOF-SIMS ion images can be used to elucidate the impurity inclusion mechanisms during the crystal growth process. For instance, the ion images of curcuminoids on the surface of crystals obtained from crystal growth (see section 3.4.) experiments suggest the same that all the three curcuminoids can take the same spot. This indicates that the inclusion of the two impurities into the bulk crystals could have occurred *via* lattice replacement. To conclude, TOF-SIMS can be used to explain the nucleation and crystal growth behaviour from an experimental stand-point.

Finally, it is worth acknowledging the limitations of the TOF-SIMS technique. The results obtained from TOF-SIMS are only semi-quantitative and careful preparation of the sample is required, followed by careful post processing of the collected data. In the present study, we created a chemical map of the curcuminoids based on the ion images of the intact molecules. In many cases, retrospective analysis of the collected data may require advanced chemometric tools and user expertise. Another major issue is the sample preparation and the results are vulnerable to surface contamination in the form of compounds adsorbed/deposited onto the sample surface from the environment. In the present study, we characterised the surface properties of the crystallised samples obtained from cooling crystallisation and crystal growth experiments. Many of the trial experiments performed with TOF-SIMS clearly indicate that the surface properties of the bulk crystals are highly vulnerable to the impurities deposited on the crystal surface from the mother liquor. To avoid this, we cleaned the final crystals obtained from the crystallisation experiments and we dried the washed crystals in a completely cleaned dryer. Additionally, we also dried one sample at a time to avoid cross contamination of the samples. In that spirit, the sample preparation time associated with TOF-SIMS is laborious but on the other hand, it provides vital information about the location of the structurally similar impurities based on the ion images of the intact molecules, which cannot be easily obtained from other analytical techniques.

Conflicts of interest

There are no conflicts to declare.

Acknowledgements

References

1 C. Heffernan, M. Ukrainczyk, J. Zeglinski, B. K. Hodnett and Å. C. Rasmuson, *Cryst. Growth Des.*, 2018, **18**, 4715–4723.

2 Z. B. Kuvadia and M. F. Doherty, *Cryst. Growth Des.*, 2013, **13**, 1412–1428.

3 K. H. Hsi, M. Kenny, A. Simi and A. S. Myerson, *Cryst. Growth Des.*, 2013, **13**, 1577–1582.

4 T. T. H. Nguyen, A. Khan, L. M. Bruce, C. Forbes, R. L. O'Leary and C. J. Price, *Crystals*, 2017, **7**, 294.

5 J. F. Banfield, S. A. Welch, H. Zhang, T. T. Ebert and R. L. Penn, *Science*, 2000, **289**, 751–754.

6 C. Heffernan, An investigation into the effect of impurities on the crystallization of curcumin, *PhD Thesis*, University of Limerick, 2019.

7 S. J. Urwin, G. Levilain, I. Marziano, J. M. Merritt, I. Houson and J. H. Ter Horst, *Org. Process Res. Dev.*, 2020, **24**, 1443–1456.

8 K. Sangwal, *Additives and Crystallization Processes: From Fundamentals to Applications*, John Wiley and Sons, 1st edn, 2007.

9 R. Boistelle and J. P. Astier, *J. Cryst. Growth*, 1988, **90**, 14–30.

10 K. V. Kumar and F. Rocha, *Surf. Sci.*, 2010, **11–12**, 981–987.

11 S. J. Urwin, G. Levilain, I. Marziano, J. M. Merritt, I. Houson and J. H. Ter Horst, *Org. Process Res. Dev.*, 2020, **24**, 1443–1456.

12 K. Sangwal, *J. Cryst. Growth*, 1993, **128**, 1236–1244.

13 S. Ottoboni, M. Chrubasik, L. M. Bruce, T. T. H. Nguyen, M. Robertson, B. Johnston, I. D. H. Oswald, A. Florence and C. Price, *Cryst. Growth Des.*, 2018, **18**, 2750–2758.

14 J. C. Vickerman and D. Briggs, *TOF-SIMS : materials analysis by mass spectrometry*, IM Publications, 2nd edn, 2013.

15 M. C. Davies and R. A. P. Lynn, *Clin. Mater.*, 1990, **5**, 97–114.

16 L. Huang, Y. Chen, L.-T. Weng, M. Leung, X. Xing, Z. Fan and H. Wu, *Anal. Chem.*, 2016, **88**, 12196–12203.

17 S. Nakano, T. Yamagishi, S. Aoyagi, A. Portz, M. Dürr, H. Iwai and T. Kawashima, *Biointerphases*, 2018, **13**, 3–403.

18 L. J. Gamble and C. R. Anderton, *Microsc. Today*, 2016, **24**, 24–31.

19 A. Henss, S.-K. Otto, K. Schaepe, L. Pauksch, K. S. Lips and M. Rohnke, *Biointerphases*, 2018, **13**, 03B410.

20 H. Liebl, *Scanning*, 1980, **3**, 79–89.

21 A. M. Belu, M. C. Davies, J. M. Newton and N. Patel, *Anal. Chem.*, 2000, **15**, 5625–5638.

22 D. J. Graham and D. G. Castner, *Mass Spectrom.*, 2013, **2**, S0014–S0014.

23 T. J. Barnes, I. M. Kempson and C. A. Prestidge, *Int. J. Pharm.*, 2011, **417**, 61–69.

24 C. Heffernan, M. Ukrainczyk, R. K. Gamidi, B. K. Hodnett and Å. C. Rasmuson, *Org. Process Res. Dev.*, 2017, **21**, 821–826.

25 H. D. Keith and F. J. Padden, *J. Appl. Phys.*, 1963, **34**, 2409–2421.

26 D. Xia, M. Ouyang, J. X. Wu, Y. Jiang, H. Piao, S. Sun, L. Zheng, J. Rantanen, F. Cui and M. Yang, *Pharm. Res.*, 2012, **29**, 158–169.

27 F. J. Padden and H. D. Keith, *J. Appl. Phys.*, 1959, **30**, 1479–1484.

28 G. Ryschenkow and G. Faivre, *J. Cryst. Growth*, 1988, **87**, 221–235.

29 A. D. Fowler, B. Berger, M. Shore, M. I. Jones and J. Ropchan, *Precambrian Res.*, 2002, **115**, 311–328.

30 L. Gránásy, T. Pusztai, G. Tegze, J. A. Warren and J. F. Douglas, *Phys. Rev. E: Stat., Nonlinear, Soft Matter Phys.*, 2005, **72**, 011605.

31 Y.-F. Chen, E. M. Woo and P.-L. Wu, *Mater. Lett.*, 2007, **61**, 4911–4915.

32 S. Tracy, D. Williams and H. Jennings, *J. Cryst. Growth*, 1998, **193**, 382–388.

33 K. Vasanth Kumar, K. A. Ramisetty, K. Renuka Devi, G. Rama Krishna, C. Heffernan, A. A. Stewart, J. Guo, S. Gadipelli, D. J. L. Brett, E. P. Favvas and Å. C. Rasmuson, *ACS Omega*, 2021, **6**, 23884–23900.

34 H. D. Keith and F. J. Padden, *J. Appl. Phys.*, 1964, **35**, 1286–1296.

35 V. B. Berzin, L. G. Katsitadze, T. V. Pilipenko, V. V. Ovcharenko and A. I. Moroshnikov, *Bioorg. Chem.*, 1996, **22**, 823–831.

36 R. Coorey and P. Håkansson, *Sri Lankan J. Phys.*, 2003, **4**, 11.

37 H. Fujimoto, T. Edura, T. Miyayama, N. Sanada and C. Adachi, *J. Vac. Sci. Technol., B: Nanotechnol. Microelectron.: Mater., Process., Meas., Phenom.*, 2014, **32**, 030604.

38 J. C. Vickerman, *Encycl. Mater. Sci. Technol.*, 2001, pp. 8624–8628.

39 S. Ferrari and B. D. Ratner, *Surf. Interface Anal.*, 2000, **29**, 837–844.